Study of ^{206}Pb by means of the ^{209}Bi$(\vec{p},\alpha)^{206}$Pb reaction

E. Gadioli, P. Guazzoni, M. Jaskóła,* L. Zetta, and G. Colombo
Dipartimento di Fisica dell'Università and Istituto Nazionale di Fisica Nucleare, via Celoria 16, I-20133 Milano, Italy

G. Graw, R. Hertenberger, D. Hofer, H. Kader, and P. Schiemenz
Sektion Physik der Universität München, D-8046 Garching, Germany

R. Neu and G. Staudt
Physikalisches Institut der Universität Tübingen, D-7400 Tübingen, Germany

(Received 9 October 1992)

The ^{209}Bi$(\vec{p},\alpha)^{206}$Pb reaction has been studied at an incident proton energy of 22 MeV using a polarized proton source and a quadrupole-dipole-dipole-dipole spectrometer. The differential cross sections and asymmetries for transitions to levels of ^{206}Pb up to an excitation energy of 5.333 MeV have been measured. Evidence for the presence of multiplets of ^{206}Pb states homologous to the parent ^{205}Tl states is discussed. The differential cross sections and asymmetries for the transitions to these homologous states are interpreted in terms of the experimental differential cross sections and asymmetries of the parent states as well as by theoretical calculations using both conventional Woods-Saxon and double-folded α-particle potentials. The differential cross sections and asymmetries for the low-energy states of ^{206}Pb which involve the pickup of the $h_{9/2}$ proton outside the closed shell are analyzed.

PACS number(s): 24.50.+g, 24.70.+s, 25.40.Hs, 27.80.+w

I. INTRODUCTION

In most cases (p,α) and $(\vec{p},\alpha)$ reactions have been studied for even-even target nuclei. For these target nuclei, only one transferred orbital and total angular momentum, l and j, contribute to the excitation of a given final state, thus greatly simplifying the theoretical calculations, usually made assuming a dominant pickup reaction mechanism.

In the case of odd-mass target nuclei, generally several l and j are allowed for a transition to a given final state. Exploiting the orthonormality of Clebsch-Gordan coefficients in evaluating the transition amplitude [1] and the conservation of parity which allows only one l for a given j, one has to consider the incoherent sum of these contributions to the measured cross sections and asymmetries. The summation of several contributions not only complicates the calculation, but also reduces the accuracy of spectroscopic information obtainable from the analysis of the experimental data.

Therefore a great advantage is gained if, for some reasons, also for odd-mass target nuclei only one l and j dominates a given transition amplitude. It was suggested previously [2] that this behavior can be observed for a number of transitions induced on near-magic target nuclei having one proton outside a completely filled magic shell, e.g., for a nucleus such as ^{209}Bi. In such cases the dominant contribution to the α spectrum results from a process in which the incident proton picks up a proton and a pair of neutrons of the nuclear core, while the valence proton outside the core acts as a spectator. Thus two parts in the spectrum can be observed: At higher excitation energies, multiplets of states are found, whose configurations result from the coupling of this spectator proton with the one-proton-hole–two-neutron-hole state excited in the core. On the other hand, at lower excitation energies some weakly excited states are observed, which are populated by the pickup of the spectator proton together with a neutron pair of the core.

In this paper we will denote the one-proton-hole–two-neutron-hole states as parent states. They are excited in (p,α) reactions on a magic target nucleus, e.g., on ^{208}Pb. These parent states and the multiplets of states observed in (p,α) reactions on a near-magic target nucleus, e.g., ^{209}Bi, originating from the coupling of these parent states with the spectator proton, will be denoted as homologous states. In many cases, instead of speaking of homologous states we will speak of homologous levels, meaning the same physical effect.

If the coupling between the parent state and the spectator proton is weak, one expects (a) the angular distributions and asymmetries for transitions to homologous states to be very similar in shape, since the processes leading to the excitation of these states are essentially the same; (b) the differential cross section for the population of a parent state to be approximately equal in magnitude to the sum of the cross sections of the transitions to the multiplet of homologous states which corresponds to the given parent state; and finally (c) the relative cross section for the population of a homologous state with spin J in a given multiplet to be proportional to $(2J+1)$. If these expectations are fulfilled, one can find the homologous states by comparing the differential cross sections and asymmetries of the (p,α) reactions induced in both target nuclei. This comparison allows one to identify unambi-

*Permanent address: Soltan Institute for Nuclear Studies, Swierk, Poland.

guously the configuration of the homologous states and therefore might prove to be a useful spectroscopic tool for nuclear states observed at relatively high excitation energies.

A low-resolution investigation of the (p,α) reaction on ^{208}Pb and ^{209}Bi, previously carried out with an unpolarized proton beam, has shown that these nuclei are most suitable to investigate this effect [2]. We now have studied the ^{208}Pb $(\vec{p},\alpha)^{205}$Tl and ^{209}Bi$(\vec{p},\alpha)^{206}$Pb reactions at 22 MeV incident energy in a high-resolution experiment. The analysis of the first reaction has been reported elsewhere [3]. In this paper we present and analyze differential cross sections and asymmetries of α-particle feeding, at the same proton energy, the multiplets of states in ^{206}Pb which are excited by the $(\vec{p},\alpha)$ reaction on ^{209}Bi and are homologous to the first five excited states in ^{205}Tl. A preliminary discussion of these data has been reported elsewhere [4]. In addition, we also analyze the differential cross sections and asymmetries of the low-lying states in ^{206}Pb (with energies less than $\approx$3.2 MeV) which are populated in processes involving the pickup of the spectator proton.

The paper is organized as follows. In Sec. II we describe the experimental procedures; in Sec. III we discuss the evidence for the presence of multiplets of ^{206}Pb states homologous to the parent ^{205}Tl states; an interpretation of the differential cross sections and asymmetries for transitions to these states is given in terms of the experimental differential cross sections and asymmetries of the parent states as well as by theoretical calculations using both double-folded and more conventional Woods-Saxon α-nucleus potentials. In Sec. IV we show and analyze the differential cross sections and asymmetries of the weakly excited low-energy states in ^{206}Pb which involve the pickup of the $h_{9/2}$ proton outside the closed shell. Finally, Sec. V is devoted to the conclusions.

II. EXPERIMENTAL SETUP

The ^{209}Bi$(\vec{p},\alpha)^{206}$Pb reaction has been studied at 22 MeV incident energy with the Munich HVEC MP tandem accelerator using the polarized ion source, a quadrupole-dipole-dipole-dipole magnetic spectrograph and the position and angle-resolving light ion detector with periodic readout [5], in a similar way as in Ref. [3]. A ^{209}Bi target with a thickness of 40 μg/cm^2 on a carbon backing of 16 μg/cm^2 thickness was used. The overall energy resolution was about 12 keV, resulting from the target energy loss.

Differential cross sections and asymmetries were measured in the range from 10° to 50° in 5° steps up to an excitation energy of about 6.5 MeV. The spectrograph solid angle was 11.04 msr, the beam current was up to 190 nA, and the up and down polarization value was 0.75.

In order to calibrate the energy scale, the α-particle spectrum measured in the ^{208}Pb$(p,\alpha)^{205}$Tl reaction with identical magnetic fields in the spectrograph was used. In this experiment a 50-μg/cm^2 ^{208}Pb target on a 18-μg/cm^2 carbon backing was used. The calibration was carried out by means of a third-order polynomial fit to the position spectrum. The quoted energies are estimated to have an uncertainty of $\pm$3 keV.

In Fig. 1 an α-particle spectrum is shown, measured at 10°, as a function of the excitation energy of ^{206}Pb. This spectrum combines measurements in several spectrograph settings, covering the energy ranges of 0–3500 and 3000–6500 keV.

The peak areas were obtained by analyzing the α-particle spectra with the code AUTOFIT using, as reference, the shape of the α-particle peak at 3.279 MeV for both spin-up and -down spectra.

In Table I the energies of the levels of ^{206}Pb measured in the present work are given together with the attributed spins and parities. These values are compared with the energies, spins, and parities of ^{206}Pb levels adopted so far [6] and with the energies, spins, and parities of the levels observed in (p,p') [7] and (d,d') [8] reactions.

The differential cross sections and asymmetries measured in this work are given in Figs. 2–5. The error bars indicate the statistical errors and are drawn only when they exceed the symbol size.

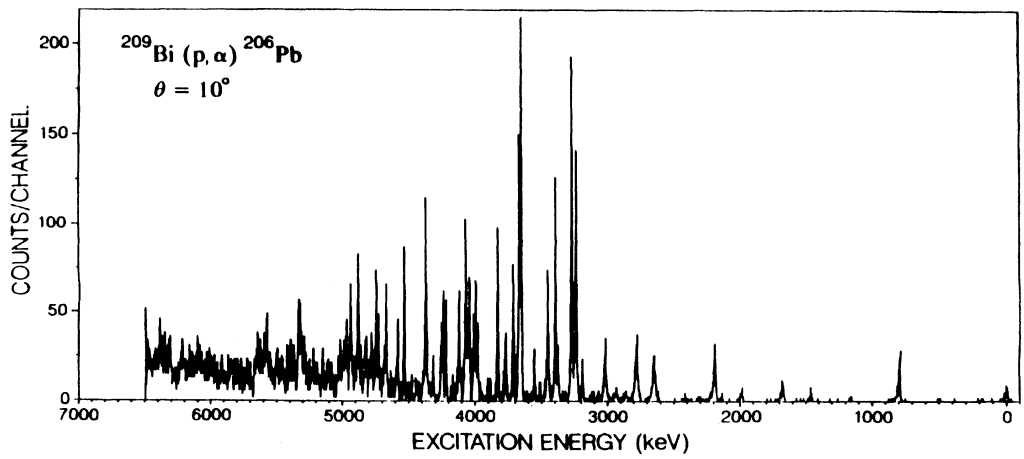

FIG. 1. Energy spectrum of α particles measured at 10°.

TABLE I. Energies, spins, and parities of ^{206}Pb levels under consideration: Adopted values [6] (columns 1,2); energies and l transfers observed in (p,p') [7] and (d,d') [8] reactions (columns 3–6); energies, spin, and parities and the numbering of levels observed in this experiment (columns 7–9). The numbers of column 9 are used to identify the experimental data given in Figs. 2–5.

Adopted levels		(p,p') reactions		(d,d') reactions		Present work levels		
E (MeV)	J^π	E (MeV)	L	E (MeV)	L	E (MeV)	J^π	Identification No.
0.0	0^+	0.0		0.0	0	0.0	0^+	1
0.803	2^+	0.803	2	0.803	2	0.806	2^+	2
1.166	0^+	1.170		1.163	(0)	1.168		3
1.340	3^+	1.344		1.340				
1.467	2^+	1.469	2	1.464	(2)	1.462		4
1.684	4^+	1.686	4	1.680	4	1.683	4^+	5
1.703	1^+	1.708						
1.784	2^+	1.787						
1.998	4^+	1.998	4	1.993	4	1.994		6
2.148	2^+	2.151	(2)			2.149		7
2.197				2.197				
2.200	7^-	2.200	7			2.200	7^-	8
2.236								
2.315	0^+					2.314		9
2.384	6^-	2.385						
2.391								
2.423	2^+	2.422	(2)			2.423		10
2.648	3^-	2.648	3	2.649	3			
2.658	9^-					2.654	9^-	11
2.782	5^-	2.782	5	2.782	(5)	2.782	5^-	12
2.826	(4^-)	2.831						
2.865	7^-	2.861				2.864		13
2.929	4^+	2.928	4	2.925	(4)			
						2.933		14
2.940	6^-							
2.960		2.960						
2.984	2^+	2.988						
3.016	5^-	3.014	5	3.014	(5)	3.016		15
3.033		3.033						
3.121	(3^+)	3.121						
3.139		3.139						
3.193	(5^-)	3.193	(5)			3.191		16
3.195	(1,2)							
3.225	6^-,7^-	3.224						
3.244	4^-					3.237	4^-	17
3.260	6^+	3.257	6	3.256		3.262		18
3.279	5^-	3.277	5	3.276		3.273	5^-	19
3.328		3.328						
3.377		3.377				3.376		20
3.403	5^-	3.399	5	3.400	5	3.399	5^-	21
						3.447		22
3.453	5^-							
3.453	4^+	3.450	4	3.450				
3.483		3.478						
						3.510		23
3.516	(4^+)	3.515	(5)					
						3.555		24
3.563	5^-	3.558	5	3.559	(5)			
3.605	2^+	3.603						
3.636	4^+							
3.655		3.655				3.653	6^-	25
						3.672	4^-	26
3.683		3.675						
3.718	3^-	3.718	3	3.719		3.716	3^-	27
3.744	1^-	3.737						
3.768	2^+					3.769		28
3.776	5^-	3.772	5	3.774	(5)			

TABLE I. (*Continued*).

Adopted levels		(*p*,*p'*) reactions		(*d*,*d'*) reactions		Present work levels		
E (MeV)	J^π	*E* (MeV)	*L*	*E* (MeV)	*L*	*E* (MeV)	J^π	Identification No.
3.778								
3.795		3.795						
3.827		3.827				3.828	$(6^-,7^-)$	29
3.847		3.847						
3.883		3.883						
3.900	(2)	3.898						
3.944								
3.957	(10^+)							
3.960	$9^-,8^+$							
3.960	6^+							
3.963	4^+	3.963	(8)					
3.971								
						3.980	2^-	30
3.989		3.980						
3.997						3.994	5^-	31
4.000								
4.005	(4^+)	4.006	(4)					
4.010						4.012		32
4.027	12^+							
4.035								
4.045		4.044	(6,7)			4.044	$(3^-,4^-)$	33
4.051								
4.066	5^-	4.059	(5)			4.064		34
4.076		4.073				4.080		35
4.100	0							
4.102	2^+	4.107	2					
4.116	2^+							
4.123	6^+	4.123	6			4.120	$(6^-,7^-)$	36
4.142	(3^-)	4.145						
4.168	(3^-)	4.168	(3)					
4.187		4.189						
4.212	1,2							
4.222	(4^+)	4.219	(4)			4.221	$(3^-,4^-)$	37
4.238	5^-	4.242	(2)			4.243	$(7^-,8^-)$	38
						4.257	$(5^-,7^-)$	39
4.290	(3^-)	4.292	(3)					
4.320	4^+					4.317	2^-	40
4.331	1^-							
4.340	(4^+)	4.333	4					
4.347	6^+	4.357	6					
						4.373		41
4.385	(5^-)	4.391	(5)					
4.410								
4.420		4.420						
4.427								
4.434								
4.459	(5^-)	4.456	(5)					
4.469		4.474	5					
4.470	(6,7)							
4.483								
4.498	$(5^-,6^+)$	4.496	(5,6)					
4.512								
4.520	9^-							
4.525								
4.534	5^-	4.534	5			4.532		42
4.575	$(7^-,8^+)$	4.580	8					
						4.584	(7^-)	43
4.595		4.595						
4.606	1^-							

TABLE I. (*Continued*).

Adopted levels		(p,p') reactions		(d,d') reactions		Present work levels		
E (MeV)	J^π	E (MeV)	L	E (MeV)	L	E (MeV)	J^π	Identification No.
4.617	(3^-)	4.614	(3)					
4.648		4.647						
4.657								
4.664	5	4.664	5					
4.675						4.673	(8^-)	44
						4.687	(2^-)	45
4.697		4.691						
4.717		4.710	(4,5)					
4.730		4.729				4.728	(9^-)	46
4.740		4.742						
						4.748		47
4.756								
4.763	1,2	4.770						
4.782	1,2					4.778		48
4.793	5	4.793	5					
4.795								
4.806	$(5^-,6^+)$	4.809	(5,6)					
						4.818		49
4.828	(7^-)	4.828	(7)			4.833	(5^-)	50
4.840	10^+							
4.848	1,2							
4.860	(6^+)	4.860	(6)			4.862	(3^-)	51
4.873		4.873				4.878	(6^-)	52
4.889	(3^-)	4.889	(3)					
4.900	(7^-)	4.901						
4.914	(3^-)	4.916	(3)			4.912		53
						4.925		54
4.939	(6^+)	4.939	(6)			4.941		55
4.966	(3^-)	4.960	(3)					
4.973	1^-					4.979		56
4.986	(3^-)	4.986	(3)					
5.007	(4^-)	5.007	(4)			5.011		57
5.025		5.025						
5.038		5.045						
5.040	10^+							
5.069		5.069						
						5.078		58
5.089	$(3^-,4^+)$	5.092	(3,4)					
5.100								
5.111	(4^+)	5.111	(4)			5.112		59
5.126		5.126						
5.134	(8^+)	5.138						
						5.149		60
5.166		5.169						
5.180								
5.195	(2^+)	5.190						
5.209		5.209						
5.236		5.227						
5.247	2^+	5.245	(3)					
5.261	3^-							
5.276	(1^-)							
		5.279						
5.282								
5.293	$(3^-,2^+)$	5.296						
5.315	(2^+)	5.309				5.317		61
5.328	$(2^+,3^-)$	5.332	(3)			5.333		62

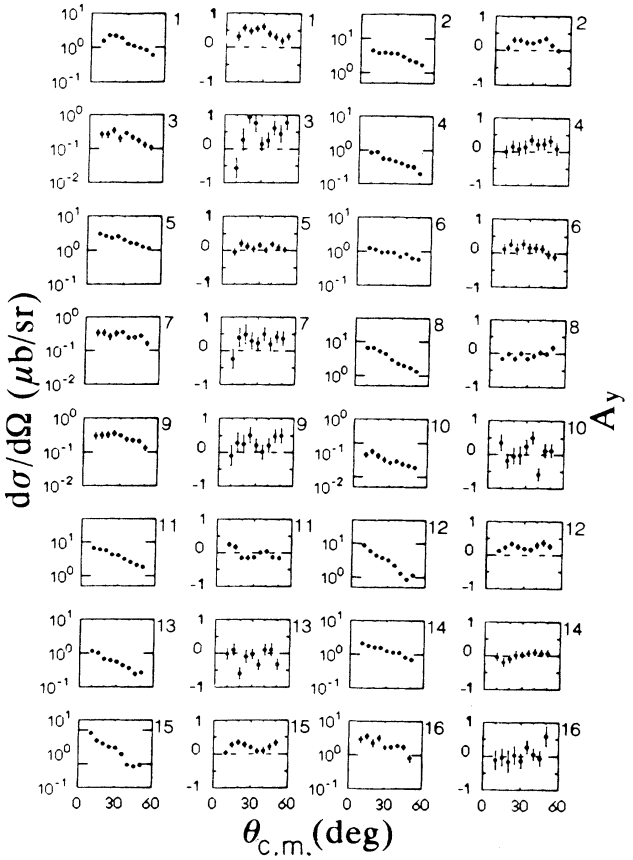

FIG. 2. Experimental angular distributions and asymmetries for levels 1–16 of Table I.

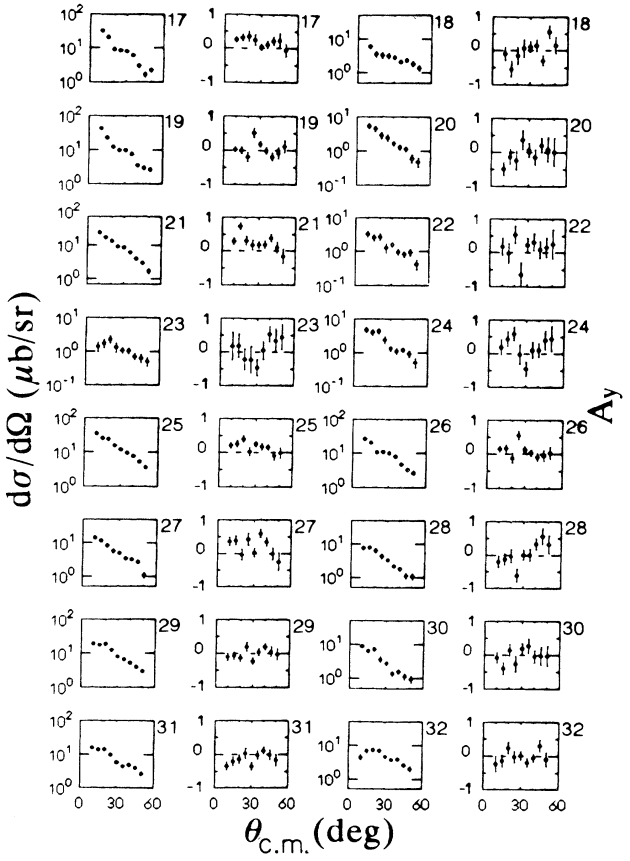

FIG. 3. Experimental angular distributions and asymmetries for levels 17–32 of Table I.

III. EVIDENCE FOR THE PRESENCE OF ^{206}Pb LEVELS HOMOLOGOUS TO THE FIRST FIVE EXCITED STATES OF ^{205}Tl

It can be seen in Fig. 1 that the ^{206}Pb levels are appreciably excited at energies above approximately 3.2 MeV. In the range up to this energy, only a few states are populated with rather weak intensity. We expect, following our previous suggestion [2], that the multiplets of levels homologous to the ^{205}Tl levels are populated starting just at an excitation energy of 3.2 MeV.

In the energy range between about 3 and 5 MeV, we expect the excitation of levels homologous to the lowest-energy levels of ^{205}Tl: namely, the $\frac{1}{2}^+$ g.s., the $\frac{3}{2}^+$ 0.204-MeV level, the $\frac{5}{2}^+$ 0.619-MeV level, the $\frac{7}{2}^+$ 0.924-MeV level, the $\frac{9}{2}^+$ 1.430-MeV level, and the $\frac{11}{2}^-$ 1.484-MeV level. The differential cross sections and analyzing powers for the ^{208}Pb$(\vec{p},\alpha)^{205}$Tl transitions to the first four states in ^{205}Tl [3] are quite different to each other (see Fig. 6). Therefore the identification of the corresponding homologous states in ^{206}Pb is somewhat easier than the identification of the levels homologous to the $\frac{9}{2}^+$ and $\frac{11}{2}^-$ states in ^{205}Tl. For these two transitions, the angular distributions of both the cross sections and asymmetries are very similar to each other. In fact, the multiplets of states in ^{206}Pb, which are homologous to the first four levels of ^{205}Tl, are rather easily identified by visual inspection of the corresponding angular distributions of the cross sections and asymmetries. These multiplets are reported in Table II.

As expected, one finds a doublet of levels in ^{206}Pb homologous to the g.s. of ^{205}Tl, a quartet for the $\frac{3}{2}^+$ state, and a sextet for the $\frac{5}{2}^+$ state. If the differential cross sections for the transitions appertaining to the same multiplet are summed, the obtained cumulative $\sigma_c(\theta)$ is in perfect agreement in both absolute value and shape with the $\sigma(\theta)$ for the transition to the homologous parent state in ^{205}Tl. This is shown in Fig. 6, where the $\sigma_c(\theta)$ for the excitation of the multiplets (solid circles) are superimposed to the differential cross sections for the excitation of the respective homologous parent states in ^{205}Tl (solid lines); a good agreement between both sets of data, respectively, can be observed. A similar agreement is also found for the asymmetries $A_y(\theta)$ (Fig. 6).

We have identified only a quintet of levels of ^{206}Pb homologous to the $\frac{7}{2}^+$ level of ^{205}Tl instead of the expected octet; however (as shown in Fig. 6), the cumulative cross section for this quintet practically coincides with that for the homologous level in ^{205}Tl. Following the experimental evidence, we are inclined to think that the two

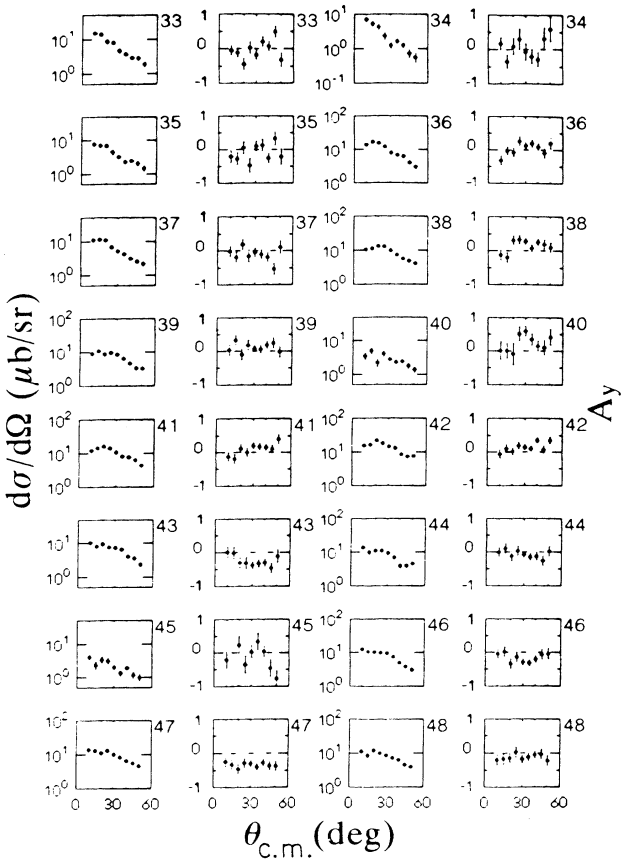

FIG. 4. Experimental angular distributions and asymmetries for levels 33–48 of Table I.

levels, at 4.373 and 4.532 MeV, might be doublets. In fact, they present a width larger than the others, in all the α-energy spectra. Moreover, their angular distributions and asymmetries allow one to consider them homologous to the $\frac{7}{2}^+$ level. So one level is still missing. This could be the 1^- member of the multiplet whose cross section is expected to be very small and consequently its observation would be difficult.

The identification of the ^{206}Pb levels homologous to the $\frac{9}{2}^+$ level of ^{205}Tl is much more uncertain because of the similarity of the expected angular distributions with those of the levels homologous to the $\frac{11}{2}^-$ state. However, a number of identifications have been made tentatively, mainly on the basis of the angular distributions of the measured asymmetries. The corresponding cumulative $\sigma_c(\theta)$ is in good agreement with that of the $\frac{9}{2}^+$ level of ^{205}Tl, as shown in Fig. 6. Likewise, allowing for the presence of doublets of levels in this case, we feel that we have identified most of the levels of the multiplet.

The identification of the levels of ^{206}Pb homologous to the $\frac{11}{2}^-$ level of ^{205}Tl appears too uncertain to provide significant information due also to the increasing density of the observed levels.

The spins of the ^{206}Pb levels homologous to the low-energy levels of ^{205}Tl are attributed on the basis of the $(2J+1)$ rule. The parities are opposite to those of the

TABLE II. Energies, spins, and parities of homologous ^{205}Tl and ^{206}Pb levels: Parent states in ^{205}Tl (columns 1,2); homologous states in ^{206}Pb (columns 3,4); adopted spin and parity values [6] (column 5).

^{205}Tl	J^π	^{206}Pb	J^π	J^π_{ad}
g.s.	$\frac{1}{2}^+$	3.273	5^-	5^-
		3.672	4^-	
0.204	$\frac{3}{2}^+$	3.237	4^-	4^-
		3.399	5^-	5^-
		3.653	6^-	
		3.716	3^-	3^-
0.619	$\frac{5}{2}^+$	3.828	$(6^-,7^-)$	
		3.980	2^-	
		3.994	5^-	
		4.044	$(3^-,4^-)$	
		4.120	$(6^-,7^-)$	
		4.221	$(3^-,4^-)$	
0.924	$\frac{7}{2}^+$	4.243	$(7^-,8^-)$	
		4.257	$(6^-,7^-)$	
		4.317	2^-	
		4.373		
		4.532		
1.430	$\frac{9}{2}^+$	4.584	(7^-)	
		4.673	(8^-)	
		4.687	(2^-)	
		4.728	(9^-)	
		4.833	(5^-)	
		4.862	(3^-)	
		4.878	(6^-)	

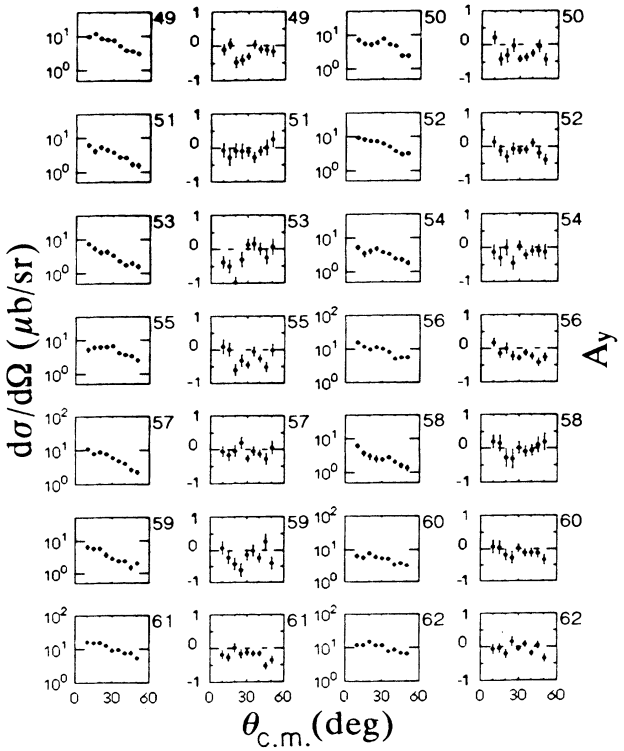

FIG. 5. Experimental angular distributions and asymmetries for levels 49–62 of Table I.

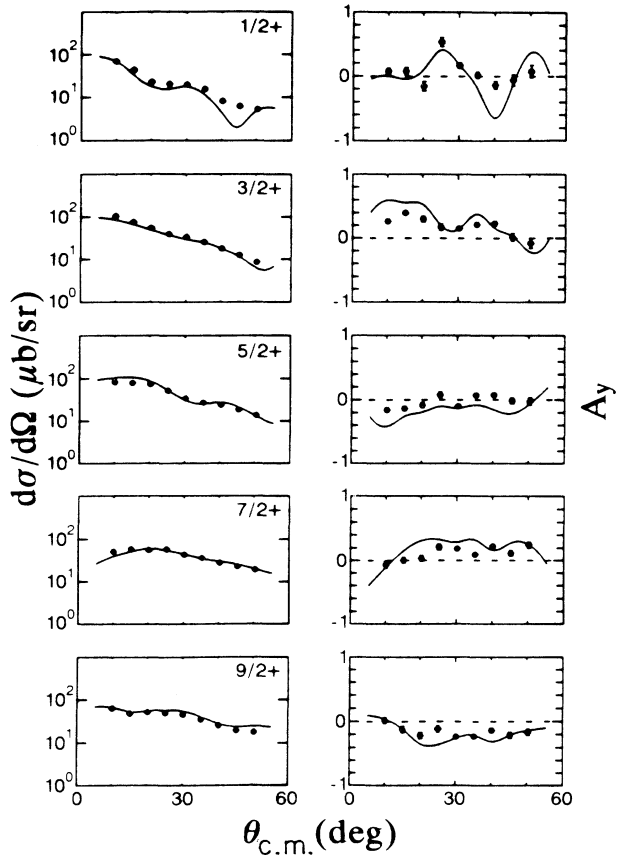

FIG. 6. Comparison of the cumulative cross sections and analyzing powers for population of the multiplets of states of ^{206}Pb, considered to be homologous to the low-lying parent states of ^{205}Tl (solid points), with the cross sections and analyzing powers for population of these ^{205}Tl states (solid lines). The J^{π} values given denote spin and parity of the parent states.

^{205}Tl levels. The comparison of the measured $\sigma(\theta)$ and $A_y(\theta)$ for the transitions to the various levels of the multiplets in ^{206}Pb (solid circles) and the angular distributions of the cross sections and asymmetries for the transitions to the corresponding parent levels in ^{205}Tl, scaled for each level i by the factor $(2J_i+1)/\sum_i(2J_i+1)$ (solid line), is shown in Figs. 7–11.

On the basis of the $(2J+1)$ criterion, we attribute spin 5^- and 4^- to, respectively, the 3.273- and 3.672-MeV levels homologous to the $\frac{1}{2}^+$ g.s. of ^{205}Tl. The first attribution coincides with the adopted spin and parity of a level reported at 3.279 MeV [6].

The spins and parities attributed to the quartet of levels homologous to the 0.204-MeV $\frac{3}{2}^+$ level of ^{205}Tl are 4^-, 5^-, 6^-, and 3^- for, respectively, the 3.237-, 3.399-, 3.653-, and 3.716-MeV levels. The first two attributions coincide with those of the levels at 3.244 and 3.403 MeV and the fourth with that of the level at 3.718 MeV reported by Helmer and Lee [6].

The spins and parities attributed to the sextet of levels homologous to the 0.619-MeV $\frac{5}{2}^+$ level of ^{205}Tl are $(6^-,7^-)$, 2^-, 5^-, $(3^-,4^-)$, $(6^-,7^-)$, and $(3^-,4^-)$ for, respectively, the 3.828-, 3.980-, 3.994-, 4.044-, 4.120-, and

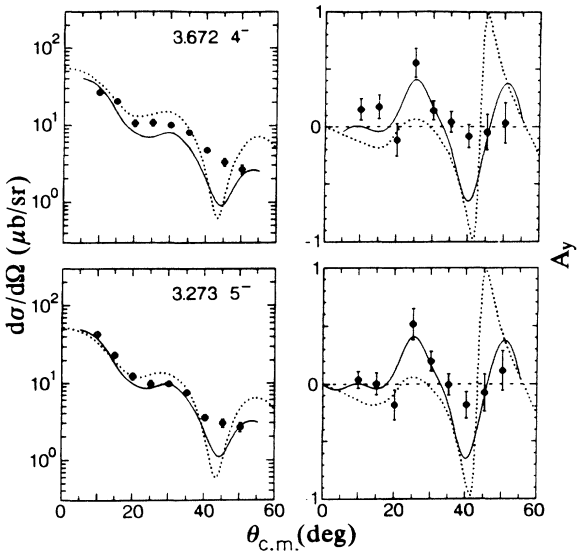

FIG. 7. Comparison of the experimental cross sections and analyzing powers for population of the doublet of levels of ^{206}Pb homologous to the $\frac{1}{2}^+$ g.s. of ^{205}Tl (solid points) with (a) the experimental cross section [scaled according to the $(2J+1)$ rule using the J values shown] and analyzing power for population of the ground state of ^{205}Tl (solid lines), and (b) the cross section and the analyzing power calculated with DWUCK5 using a double-folded α-particle potential (dotted lines).

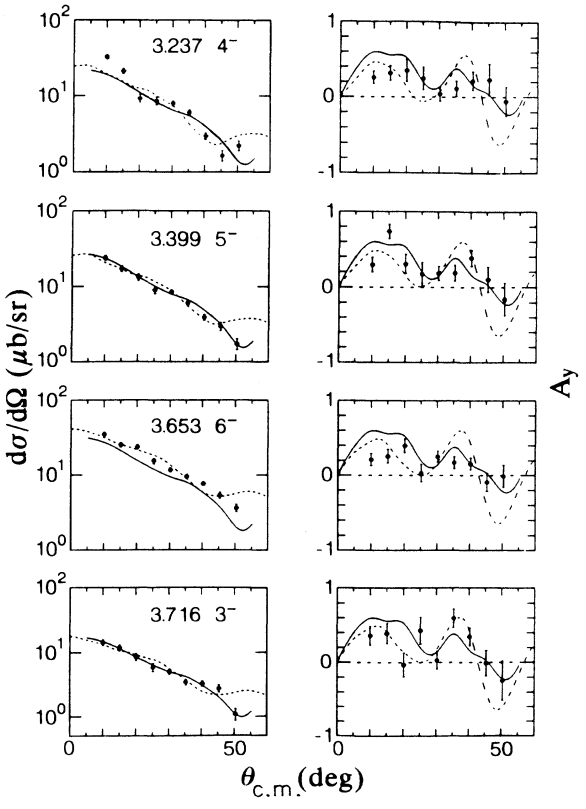

FIG. 8. Same as Fig. 7 but for the quartet of levels of ^{206}Pb homologous to the $\frac{3}{2}^+$ 0.204-MeV level of ^{205}Tl.

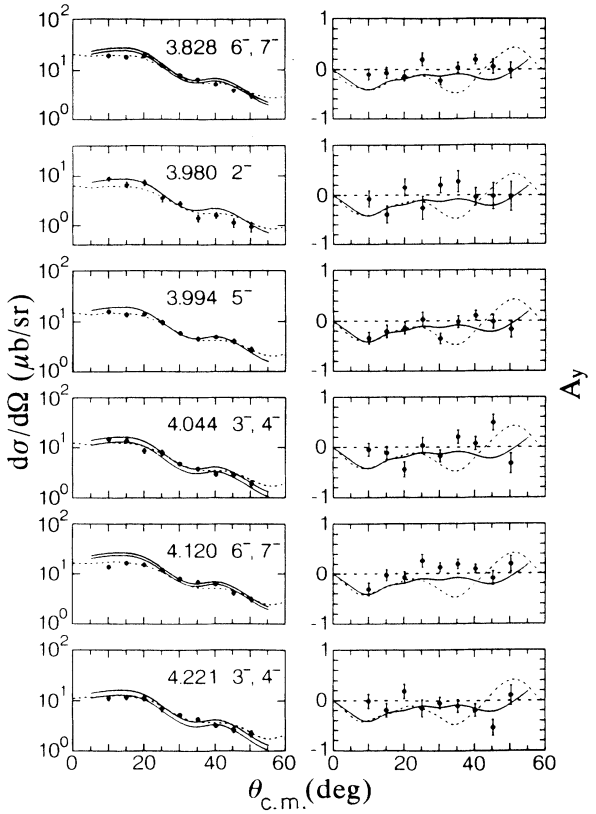

FIG. 9. Same as Fig. 7 but for the sextet of levels of ^{206}Pb homologous to the $\frac{5}{2}^+$ 0.619-MeV level of ^{205}Tl.

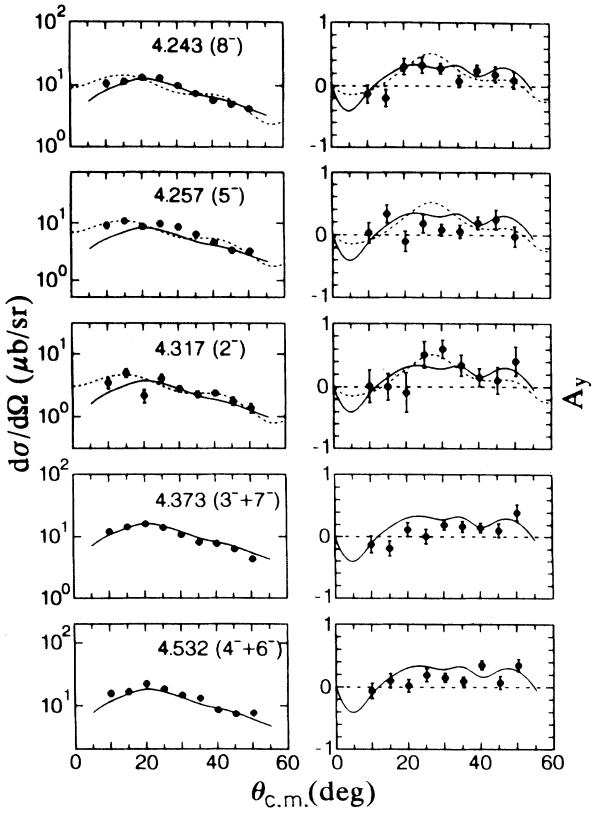

FIG. 10. Same as Fig. 7 but for the levels of ^{206}Pb considered to be homologous to the $\frac{7}{2}^+$ 0.924-MeV level of ^{205}Tl. In this case, because of the possible presence of multiplets at 4.373 and 4.532 MeV of excitation energy, the spin attributions are more doubtful than in other cases and the values given are tentative.

4.221-MeV levels. There are no adopted values of spin and parity for the first three levels [6]. The fourth might be a member with $J \leq 4$ of a suggested doublet at 4.045 MeV [6]. There are spin and parity assignments for levels with energy very near to that of the last two levels, respectively, 4.123 and 4.222 MeV. To the first of them, a J^π value of 6^+ is attributed, which results from the analysis of the ^{206}Pb(p,p')^{206}Pb reaction [9]. Since it is rather difficult to distinguish between a transferred $L=6$ or 7 in an inelastic scattering experiment, this level might coincide with the one we observe (attributing $J^\pi=7^-$). The second (4.222-MeV) level has been found in the ^{208}Pb(p,t)^{206}Pb reaction [10]. A J^π value of 4^+ is attributed. Since in a (p,t) experiment the excitation of states with a two-neutron-hole configuration is preferred, this level most probably cannot coincide with that we observe, if we identify the 4.221 level as one of those homologous to the $\frac{5}{2}^+$ state in ^{205}Tl.

As mentioned before, we have identified only a quintet of levels of ^{206}Pb which may with certainty considered to be homologous of the $\frac{7}{2}^+$ 0.924-MeV level of ^{205}Tl. In this case the attribution of spins is more doubtful than in the other cases for the possible presence of two multiplets at 4.373 and 4.532 MeV of excitation energy. Thus the set of attributions shown in Fig. 10 is tentative and each spin value given could be substituted by a value differing by one unit. It seems improbable that the spin of the 4.243-MeV level could be as low as 5^- as that of the level at 4.238 MeV reported on the adopted level scheme [6]. The presumed doublet at 4.532 MeV which might comprise two levels with spins 4^- and 6^- could coincide with the level at 4.534 MeV reported on the adopted level scheme with spin 5^- attributed on the basis of a (p,p') reaction [7]. These levels are also reported in Table II where only the possible spin of the singlets is indicated.

The spins and parities of the levels which are interpreted as homologous to the $\frac{9}{2}^+$ state are likewise reported in Table II. It is difficult to decide if some of these levels coincide with levels already reported on the adopted level scheme [6] since some of the spin and parity attributions made by a (p,p') reaction [7] appear very uncertain. Among the levels we observe, those that probably were not previously seen are the 4.673- and 4.728-MeV levels. In fact, the 4.675- and 4.730-MeV states reported in the adopted level scheme are expected to have $J \leq 4$, which results from the observed γ transition rates [6].

For the transitions populating the homologous states in ^{206}Pb, distorted wave Born approximation (DWBA) analyses have been performed assuming a triton pickup mechanism. The differential cross sections and asymmetries have been calculated using the finite-range code DWUCK5 [11]. For the description of the elastic α scattering in the exit channel, we have used both conventional Woods-Saxon and double-folded optical potentials. A de-

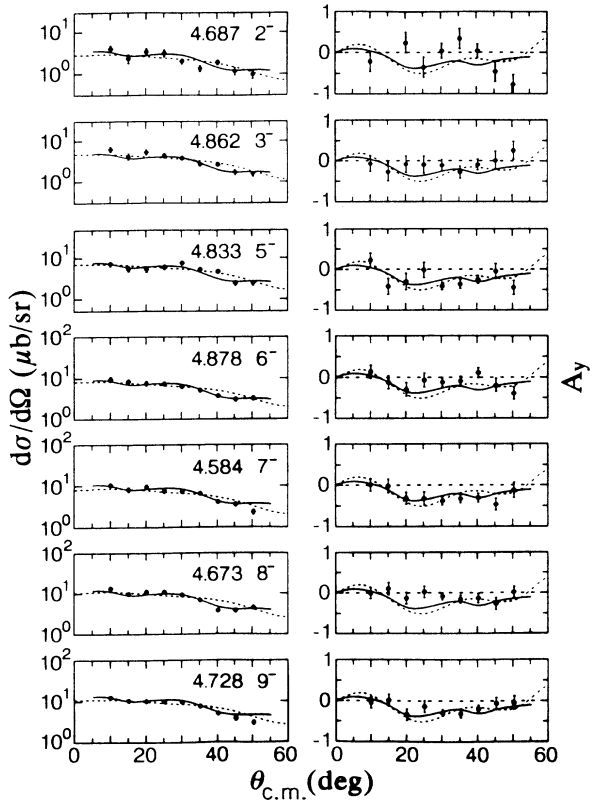

FIG. 11. Same as Fig. 7 but for a septet of levels of ^{206}Pb considered to be homologous to the $\frac{9}{2}^+$ 1.430-MeV level of ^{205}Tl.

tailed description of the folding procedure is given in Ref. [3]. The optical model parameters for the proton and the α-particle elastic scattering as used in the Woods-Saxon parametrization and the geometric parameters for evaluating the bound-state wave function of the transferred triton cluster are the same as used in Ref. [3]. They are summarized in Table III. In the case where a double-folded α-nucleus potential is used, we obtained the parameters of this potential together with those for the bound-state potential by fitting the calculated cross sections of the ground-state transition to the experimental ones. This transition is characterized by a unique l transfer. The potential parameters obtained in this way only slightly differ from the values obtained in the analysis of the ^{208}Pb$(\vec{p},\alpha)$ ^{205}Tl reaction [3]. They are given in Table IV.

In order to calculate the differential cross sections and analyzing powers shown in Figs. 7–11, for each transition only a single l transfer was used, namely, that one which is given by the transition to the corresponding parent state. That means that we used the same parameters and quantum numbers (with exception of the excitation energy) when calculating the transitions to the homologous state of a given multiplet.

In all cases the agreement between the calculated and experimental data is better when using a folding instead of a Woods-Saxon α-nucleus optical potential. Therefore in Figs. 7–11 the experimental data are only compared with the results of the finite-range DWBA calculations using the double-folding potential in the α channel. The calculated cross sections are normalized to the experimental ones separately for each transition. For transitions within the same multiplet, the normalization factors obtained have been found to be proportional to $(2J+1)$ within the expected accuracy.

The predictions of DWUCK5 (dotted lines) agree very well with the experimental data. In many but not all the cases, the DWBA calculations reproduce the data with a similar accuracy as obtained in the comparison of the data with the experimental cross sections and analyzing powers for the transitions to the corresponding parent states in ^{205}Tl (solid lines).

Concluding the results of this section, it can be stated that the concept of homologous states as suggested previously [2] is largely confirmed. An interesting consequence of homology is the fact that states in ^{206}Pb with the same spin and parity but which are members of different multiplets and therefore are homologous to different parent states in ^{205}Tl must have a different dominant configuration. Therefore the corresponding differential cross sections and analyzing powers are dissimilar as shown for transitions to 5^- states in Fig. 12(a). This violates the generally accepted rule for (p,α) reactions [12] that α's feeding states with the same J^π have nearly the same $\sigma(\theta)$ and $A_y(\theta)$. This rule holds for transitions to ^{206}Pb states which are not homologous to ^{205}Tl states as shown in Fig. 12(b).

IV. ANALYSIS OF THE TRANSITIONS INVOLVING THE PICKUP OF THE $h_{9/2}$ PROTON

As mentioned above, a number of low-energy levels with excitation energies $E_x \lesssim 3.2$ MeV are found to be weakly excited as it is possible to see in Fig. 1. These states may be populated by picking up the $h_{9/2}$ proton outside the closed shell.

In the following we discuss those with relatively larger cross sections. In order to analyze the observed cross sections and analyzing powers, we have no *a priori* argu-

TABLE III. Optical model parameters for the incident proton and the emitted α particle (Woods-Saxon parametrization) and geometrical parameters for the triton bound state.

	V (MeV)	r_V (fm)	a_V (fm)	W (MeV)	W_D (MeV)	r_W (fm)	a_W (fm)	$V_{s.o.}$ (MeV)	$r_{s.o.}$ (fm)	$a_{s.o.}$ (fm)	r_c (fm)
p	53.75	1.219	0.743		10.93	1.302	0.654	6.04	1.064	0.738	1.18
α	177.3	1.342	0.569	15.6		1.342	0.569				1.30
t		1.255	0.5								

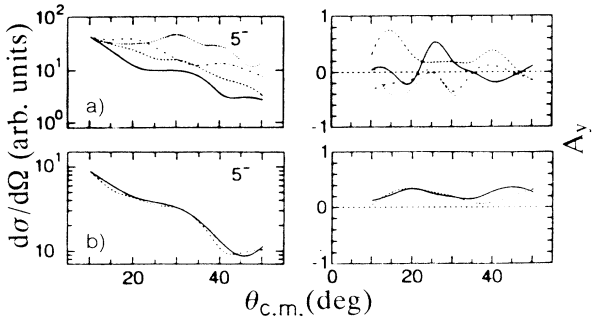

FIG. 12. Comparison of the angular distributions of cross sections and asymmetries for transitions to levels of ^{206}Pb with $J^{\pi}=5^{-}$. In the upper part (a) of the figure, the comparison is made for the transitions to the 3.273-MeV (solid line), the 3.399-MeV (dashed line), the 3.994-MeV (dot-dashed line), and the 4.833-MeV (dotted line) levels which are considered to be homologous to the g.s., the 0.204-, 0.619-, and 1.430-MeV states of ^{205}Tl, respectively. In the lower part (b), the comparison is made for the transitions to the 2.782-MeV (solid line) and the 3.016-MeV (dashed line) level which are not homologous to the ^{205}Tl levels. In order to make the comparison easier, the experimental angular distributions are given as lines and normalized to the same value at 10°.

ment to identify a dominant configuration. Therefore we calculated the cross sections and analyzing powers by adding incoherently the contributions of all the allowed j,l transfers. The various contributions were weighted with spectroscopic factors which were evaluated in the framework of the semimicroscopic model [13]. Here the primary wave-function components of the two-neutron configuration given in Ref. [6] have been used. The quantum numbers l,n,j of the transferred triton and those of the pair of picked up neutrons, $\bar{N},\bar{J}$, are given in Table V together with the corresponding spectroscopic factors.

In a first step of the analysis, DWBA calculations have been performed in a zero-range approximation applying the code DWUCK4 [11], because in its present version DWUCK5 gives unreasonably high absolute cross sections for $l \geq 10$. Woods-Saxon and double-folding α-nucleus optical potentials were used. The results of these calculations are shown in Fig. 13 as dotted and solid lines, respectively. For both kinds of α optical potentials, the theoretical results reproduce rather satisfactorily the experimental data for the transitions to the 0^{+} and 2^{+} states. But the agreement starts to become unsatisfactory for the transition of the 4^{+} state and is further deteriorated for the transitions to the negative-parity states.

One immediately recognizes that the high l transfer dominates the incoherent sum of these transitions and that the disagreement is due to these contributions. Therefore, in a second step, two kinds of calculations were carried out in which these contributions ($l=9$ in the case of the 4^{+} and $l \geq 8$ in the case of the negative-parity states) were cut off. The first one was made in a zero-range approximation using a Woods-Saxon potential, the second one in finite range using a double-folded α potential. In Fig. 14 the results of these calculations are given as dotted and solid lines, respectively. As can be seen, now the agreement between the experimental data and

TABLE IV. Normalization factor λ_f for the double-folded α-nucleus potential, the parameters of the imaginary Woods-Saxon α-nucleus potential used together with the double-folded real potential, and the geometrical parameters for the triton bound state.

E_{reac} (MeV)	λ_f	W (MeV)	r (fm)	a (fm)
22	1.179	7.64	1.613	0.724
	cluster form factor		1.314	0.944

the calculations is clearly improved and rather good.

We also made attempts to identify one possible j,l pair being dominant also for the transitions to these states. But the results were rather unsatisfactory since it appeared as impossible to obtain a good description of both the cross sections and the asymmetries.

Finally, an attempt was made applying the microscopic model in calculating the transfer form factor. In this model the form factor was constructed by the superposition of three individual single-particle wave functions. In our case these wave functions are the $h_{9/2}$-proton function and the function for the two neutrons which are

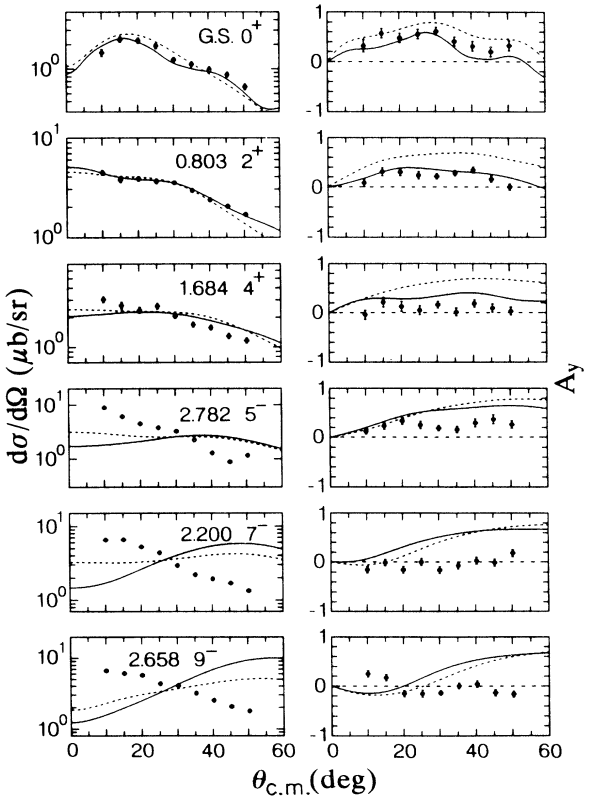

FIG. 13. Comparison of the experimental cross sections and analyzing powers for population of six low-lying levels of ^{206}Pb (with excitation energy and spin given) whose excitation involves the pickup of the $h_{9/2}$ proton outside the closed shell (solid points) with the results of DWBA calculations in a zero-range approximation using Woods-Saxon (dotted lines) and double-folded α potentials (solid lines).

determined by their suggested dominant configuration [6]. But up to now, to our knowledge, the microscopic spectroscopic factors for the different l and j transfers are unknown. Therefore we had to use again the spectroscopic factors given by the semimicroscopic model [13]. Though the shape of the microscopic form factor in the nuclear interior is very different to that of the cluster form factor, the calculations using both kinds of form factors led to very similar results with regard to the angular distributions of the (p,α) transitions. That means that the (p,α) reaction under consideration is mainly sensitive to the exponential tail of the form factor, which indeed is equal for both the cluster and microscopic calculations. This result shows that for such heavy systems the cluster

TABLE V. Summarization, for the transitions to the ground state and to five excited states in ^{206}Pb (whose spin and parity values are given in column 2), of the quantum numbers n,l,j of the transferred triton (column 3), the harmonic oscillator quanta NQ_1 and NQ_2 of the proton and the two-neutron pair, respectively (columns 4 and 5), the radial quantum number $\bar{N}$ and the angular momentum $\bar{J}$ of the two-neutron pair (columns 6 and 7), and the spectroscopic amplitudes [13] used for evaluating the contributions of the different l and j to the transitions.

E_{exc} (MeV)	J^π	l,n,j	NQ_1	NQ_2	$\bar{N}$	$\bar{J}$	$[S^{nlj}_{j_\gamma,\bar{N}\bar{J}}]^{1/2}$
0.000	0^+	5,5,9/2	5	10	5	0	0.0953
0.803	2^+	3,6,5/2	5	10	4	2	0.0338
		3,6,7/2					0.0083
		5,5,9/2					0.0412
		5,5,11/2					0.0099
		7,4,13/2					0.0841
1.684	4^+	1,7,1/2	5	10	3	4	0.0132
		1,7,3/2					0.0080
		3,6,5/2					0.0149
		3,6,7/2					0.0087
		5,5,9/2					0.0217
		5,5,11/2					0.0102
		7,4,13/2					0.0386
		7,4,15/2					0.0124
		9,3,17/2					0.0986
2.782	5^-	0,8,1/2	5	11	3	5	0.0095
		2,7,3/2					0.0084
		2,7,5/2					0.0081
		4,6,7/2					0.0121
		4,6,9/2					0.0086
		6,5,11/2					0.0194
		6,5,13/2					0.0102
		8,4,15/2					0.0368
		8,4,17/2					0.0127
		10,3,19/2					0.0987
2.200	7^-	2,7,5/2	5	11	2	7	0.0074
		4,6,7/2					0.0049
		4,6,9/2					0.0063
		6,5,11/2					0.0086
		6,5,13/2					0.0072
		8,4,15/2					0.0161
		8,4,17/2					0.0095
		10,3,19/2					0.0362
		10,3,21/2					0.0136
		12,2,23/2					0.1176
2.658	9^-	4,6,9/2	5	11	1	9	0.0043
		6,5,11/2					0.0028
		6,5,13/2					0.0040
		8,4,15/2					0.0056
		8,4,17/2					0.0052
		10,3,19/2					0.0125
		10,3,21/2					0.0079
		12,2,23/2					0.0338
		12,2,25/2					0.0134
		14,1,27/2					0.1397

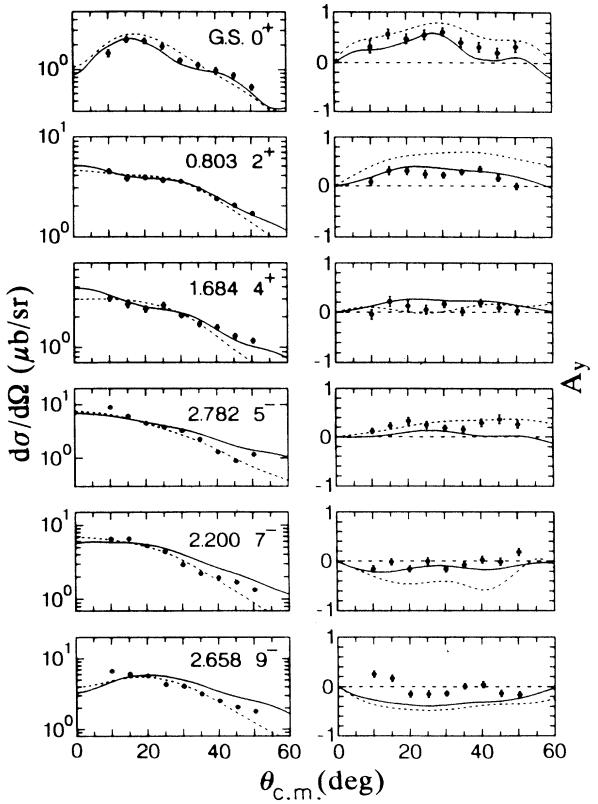

FIG. 14. Same as Fig. 13 but with the results of DWBA calculations in a zero-range approximation [using a Woods-Saxon α potential (dotted lines)] and in finite range [using a double-folded α potential (solid lines)]. In both calculations contributions with higher l transfer are cut off (see text).

approximation is justified. But the necessity to cut off the higher l transfers in order to fit the experimental data continues to be an unsolved problem.

V. CONCLUSIONS

In the case of (p,α) reactions on target nuclei with only one proton outside a completely filled magic shell, two contributions to the spectrum of the residual nucleus can be observed: The first one originates from the pickup of the proton outside the closed shell, but the dominant one is that of processes in which the incident proton picks up a proton of the core, while the extra proton acts as a spectator.

By the first process, the lowest-energy states of the residual nucleus are excited. These low-energy (0–3 MeV) states of ^{206}Pb are analyzed in the framework of DWBA employing a double-folded α potential and using the semimicroscopic model, adding incoherently the individual j,l transfer components. Because of the big number of three-particle configurations involved, the analysis is more complicated (only the transitions to 0 spin levels have a unique angular momentum transfer). The calculations indicate that, especially in the case of transitions to negative-parity states, a cutoff on higher l transfers (otherwise allowed by spin and parity conservation) improves the agreement with the data.

The analysis of the differential cross sections and asymmetries of the lowest-energy states of ^{206}Pb seems to suggest that the contributions with the highest l transfers to the transition amplitude should be greatly reduced with respect to that given by DWBA calculations using the spectroscopic factors evaluated in the framework of the semimicroscopic model.

The second process favors, at higher energies, the excitation of multiplets of homologous states whose configuration results from the coupling of the proton outside the closed shell with the one-proton-hole–two-neutron-hole states excited in the core.

This study shows that the homology concept constitutes a powerful spectroscopic tool, allowing the identification of the spin, parity, and dominant configuration of a larger number of levels with relatively high excitation energy. For the transitions to these states, a separate theoretical analysis of the differential cross sections and analyzing powers is not required once one knows the experimental data together with the DWBA analyses of the transition to corresponding parent states. The homology concept is not restricted to the cases we consider here, even if the large difference in energy between the levels of the multiplets of ^{206}Pb and the parent levels in ^{205}Tl makes this case particularly significant. It is worth mentioning that a recent study of the ^{209}Bi$(d,t)^{208}$Bi reaction also showed a clear multiplet structure originating from the coupling of the $h_{9/2}$ proton of ^{209}Bi with neutron holes in the magic shell [14].

[1] G. R. Satchler, *Direct Nuclear Reactions* (Oxford University Press, New York, 1983).
[2] E. Gadioli, E. Gadioli Erba, R. Gaggini, P. Guazzoni, P. Michelato, A. Moroni, and L. Zetta, Z. Phys. A **310**, 43 (1983).
[3] E. Gadioli, P. Guazzoni, S. Mattioli, L. Zetta, G. Graw, R. Hertenberger, D. Hofer, H. Kader, P. Schiemenz, R. Neu, H. Abele, and G. Staudt, Phys. Rev. C **43**, 2572 (1991).
[4] E. Gadioli, P. Guazzoni, L. Zetta, G. Graw, R. Hertenberger, D. Hofer, H. Kader, and P. Schiemenz, in *Proceedings of the 6th International Conference on Nuclear Reaction Mechanisms,* Varenna, 1991, edited by E. Gadioli (Ricerca Scientifica ed Educazione Permanente, Milano, 1991), Suppl. No. 84, p. 785.
[5] H. Wessner, R. Hertenberger, H. Kader, and G. Graw, Nucl. Instrum. Methods A **286**, 175 (1990).
[6] R. G. Helmer and M. A. Lee, Nucl. Data Sheets **61**, 93 (1990).
[7] J. E. Finck, G. M. Crawley, J. A. Nolen, and R. T. Kouzes, Nucl. Phys. **A407**, 163 (1983).
[8] J. Ungrin, R. M. Diamond, P. O. Tjöm, and B. Elbek, Dan. Vidensl., Selsk., Mat.-Fys. Medd. **38**, No. 8 (1971).
[9] W. A. Lanford, Phys. Rev. C **16**, 988 (1977).
[10] H. Wienke, H. P. Blok, J. F. A. Van Hienen, and J. Blok, Nucl. Phys. **A442**, 397 (1985).

[11] P. D. Kunz, University of Colorado, computer codes DWUCK4 and DWUCK5 (unpublished).
[12] P. E. Hodgson and E. Gadioli, Rep. Prog. Phys. **52**, 247 (1989).
[13] J. W. Smits and R. H. Siemssen, Nucl. Phys. **A261**, 385 (1976); J. W. Smits, Kernfysisch Versneller Instituut, Groningen, Report No. 104, 1977.
[14] H. Kader, H. Clement, G. Eckle, G. Graw, R. Hertenberger, F. Merz, and P. Schiemenz, J. Phys. Soc. Jpn. Suppl. **55**, 706 (1986).